Provided for non-commercial research and education use.
Not for reproduction, distribution or commercial use.

This article appeared in a journal published by Elsevier. The attached copy is furnished to the author for internal non-commercial research and education use, including for instruction at the authors institution and sharing with colleagues.

Other uses, including reproduction and distribution, or selling or licensing copies, or posting to personal, institutional or third party websites are prohibited.

In most cases authors are permitted to post their version of the article (e.g. in Word or Tex form) to their personal website or institutional repository. Authors requiring further information regarding Elsevier's archiving and manuscript policies are encouraged to visit:

http://www.elsevier.com/copyright

Author's personal copy

Journal of Quantitative Spectroscopy & Radiative Transfer 113 (2012) 1905–1912

Contents lists available at SciVerse ScienceDirect

Journal of Quantitative Spectroscopy & Radiative Transfer

journal homepage: www.elsevier.com/locate/jqsrt

Effective line strengths of *trans*-nitrous acid near 1275 cm^{-1} and *cis*-nitrous acid at 1660 cm^{-1}

B.H. Lee [a,*], E.C. Wood [b,c], J. Wormhoudt [b], J.H. Shorter [b], S.C. Herndon [b], M.S. Zahniser [b], J.W. Munger [a]

[a] Harvard University, School and Engineering and Applied Sciences, 20 Oxford Street, Cambridge, MA 02138, USA
[b] Aerodyne Research, Inc., Center for Atmospheric and Environmental Chemistry, Billerica, MA 01821, USA
[c] Now at University of Massachusetts at Amherst, Department of Public Health, MA 01003, USA

ARTICLE INFO

Article history:
Received 3 April 2012
Received in revised form
30 May 2012
Accepted 3 June 2012
Available online 13 June 2012

Keywords:
Nitrous acid
Effective line strength
Mid-infrared
Quantum cascade laser

ABSTRACT

We determined the effective line strengths of the *trans* conformer of nitrous acid (HONO) near 1275 cm^{-1} (R-branch of ν_3 mode, N–O–H bend) and of the *cis* conformer at 1660 cm^{-1} (R-branch of ν_2 mode, N=O stretch), both at a spectral resolution of 0.001 cm^{-1} by tunable infrared laser differential absorption spectroscopy (TILDAS) utilizing continuous-wave quantum cascade (cw-QC) lasers. Absorbance of one conformer was measured while simultaneously quantifying the mixing ratio of total HONO by catalytic conversion to nitric oxide (NO) followed by calibrated absorption spectroscopy. Line strengths obtained here are consistent with previously reported band strengths for the *trans* conformer but are lower by a factor of approximately 2.4 for the *cis* conformer.

© 2012 Elsevier Ltd. All rights reserved.

1. Introduction

Nitrous acid (HONO) is a short-lived atmospheric reservoir of nitric oxide (NO) and the hydroxyl radical (OH). Photolysis of HONO–subsequent to formation by a pathway not involving OH or the hydroperoxyl radical (HO_2)–represents a net source of HO_x ($=OH+HO_2$), collectively, one of the main drivers of atmospheric oxidation. Nighttime buildup beneath the boundary layer due to combustion emissions and heterogeneous reaction of nitrogen dioxide (NO_2) provides the dominant source of reactivity in the early morning [1,2]. Recent reports of HONO levels exceeding those expected at photostationary state suggest a secondary daytime source that may constitute a significant portion of the daily HO_x budget in urban [3–5], rural [6–9] and remote [10–12] atmospheres. In indoor environments, combustion from cooking directly releases HONO and NO_x ($=NO+NO_2$) [13], which react to generate additional HONO [14]. At enhanced levels (from few part-per-billion to several hundred ppb), HONO by itself is a minor lung and eye irritant [15,16]. Reactions with amines present in the gas phase [17] and as residue on surfaces previously exposed to cigarette smoke yield carcinogenic nitrosamines, the effect of which has been commonly called "third-hand" smoke [18]. However, the chemical mechanism, rate and nature of the substrate on which production takes place remain uncertain.

Many HONO measurement techniques rely on wet-chemical extraction, by which gaseous HONO is captured in liquid form, derivatized then quantified via photometry or chromatography [19–22]. Though offering near part-per-trillion (ppt) sensitivity, they are potentially prone to chemical interferences and have not always shown good agreement with optical techniques [23,24]. Absorption spectroscopy – applied previously in open-path [1–3,25] and enclosed cell [26–31] systems to measure ambient air

* Corresponding author. Tel.: +1 617 496 6246.
E-mail addresses: hwanlee@fas.harvard.edu, avenuel2lbj@gmail.com (B.H. Lee).

0022-4073/$ - see front matter © 2012 Elsevier Ltd. All rights reserved.
http://dx.doi.org/10.1016/j.jqsrt.2012.06.004

Author's personal copy

and combustion exhaust – offers a more direct method with greater specificity. However, the fundamental rotational-vibrational transitions of HONO in the mid-infrared spectral region are not accurately represented in any comprehensive linelist [32,33].

We report *effective* line strengths – the absorbance of light by one conformer per unit column density of total (*cis*+*trans*) HONO – determined for the *cis* conformer at 1660 cm^{-1} and the *trans* near 1275 cm^{-1} at 303 K. The *absolute* line strengths – absorbance of light per unit column density of that particular conformer – could be calculated given the *cis-trans* equilibrium constant, but the accuracy would be limited by large uncertainty in equilibrium constant [34]. The effective strength, along with line position and air-broadened halfwidth at half-maximum, γ_{air} (cm^{-1} atm^{-1}), provide the necessary parameters to quantify the concentration of total HONO by TILDAS. As thermal equilibrium between the two conformers via isomerization occurs nearly instantaneously ($\sim 10^{-12}$ s), maintaining the sample at a constant temperature for a few seconds ensures accurate total HONO quantification that is independent of thermal changes in the ambient atmosphere. We compare these results to previous effective band strength studies and discuss optimal spectral regions in which to measure HONO.

2. Experimental methods

Fig. 1 is a schematic of the experimental setup. Concentrated gaseous HONO was introduced into the sample cell of a dual cw-QC laser TILDAS system, in which the absorbance of *cis*-HONO (1659.25–1660.10 cm^{-1}; Alpes Lasers) and NO_2 (1604.56 cm^{-1}; Alpes Lasers) were simultaneously measured over an absorption path length of 210 m at reduced pressures. Total HONO at the same time was quantified via complete reduction of the sub-sampled mixture by molybdenum catalysis (TEI) to NO, which was continuously measured by a calibrated single pulsed-QC laser TILDAS instrument. Other reducible nitrogen oxide species that may have been generated along with HONO were accounted for by monitoring the NO mixing ratio prior to conversion by O_3-chemiluminescence (ThermoElectron 42i), and NO_2 by absorption spectroscopy. Additions were conducted over a range of cell pressures (6–70 Torr) to

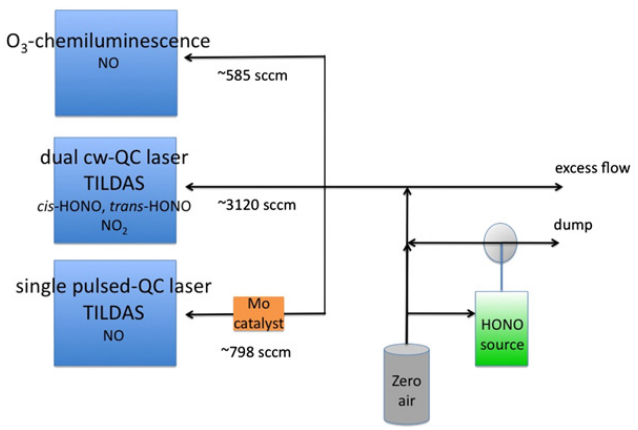

Fig. 1. Schematic of the instrumental setup.

determine γ_{air}. The dual-laser instrument was then reconfigured to concurrently measure the absorbance of both *cis* and *trans* conformers. HONO was again introduced at various cell pressures. The effective line strength and γ_{air} of the *trans* conformer (1273.38–1273.47 cm^{-1}; 1273.57–1273.62 cm^{-1}; 1274.26–1274.36 cm^{-1}; 1275.74–1275.84 cm^{-1}; Hamamatsu Photonics) was determined from the total HONO value obtained using the previously determined *cis* conformer absorption parameters.

Laser temperature control, data acquisition and spectral fitting for the laser-based systems were controlled by the software TDLWintel (Aerodyne Research, Inc.). Thermoelectrically cooled QC lasers were spectrally tuned by providing them with a programmable current ramp from a high-compliance source (ILX Lightwave) to induce a milli Kelvin-scale temperature change to tune the output light over a range of approximately 0.2 cm^{-1}. The QC lasers for both HONO conformers and NO_2 were scanned at a rate of 150 Hz (a factor of approximately 10 slower than typical operational conditions) to ensure line shape symmetry. The instrumental line widths for all three lasers were less than the 0.001 cm^{-1} spectral resolution. This was determined by scanning nearby lines of water vapor, for which absorption parameters are well known [33], at cell pressures below 2 Torr to minimize collisional broadening. Details regarding the optical layout, signal detection and sensitivity of the spectrometers are provided elsewhere [27,35].

Gas additions typically lasted between 30 and 120 s, over which the mixing ratios (and spectra) were averaged in time to reduce the variance of the final values used in the line strength calculations, described below. Flow rates were maintained to ensure sufficient mixing and to minimize residence times inside tubing and sample cells. Perfluoroalkoxy tubing was utilized and the sample cells of the TILDAS systems were treated with a siloxyl coating to reduce surface chemistry. Fig. 2a shows a brief time series of mixing ratios when NO_2 generated from a permeation device (Valco Instruments Co. Inc.) was introduced. The agreement between NO_2 quantified directly with the QC laser using HITRAN absorption parameters [33] and NO resulting from catalytic conversion (Fig. 2a), exhibits the purity of the laser mode. We also observed agreement in water vapor measurements between the two QC lasers at 1605.675 cm^{-1} and 1660.467 cm^{-1} (not pictured), establishing the laser mode purity of the *cis*-HONO laser. Moreover, additions of varying levels of NO_2 from a tank source and its absence downstream of the catalytic converter demonstrated complete conversion efficiency. We assume unity efficiency in reduction for HONO as well, as previously reported [36].

The single-channel TILDAS system used to quantify the post-conversion NO mixing ratio was calibrated using a NO tank source (Scott Specialty, 34.6 ppm $\pm$ 1%), which tested to within 1% of another NO tank (Airgas "Primary Standard", 250.6 ppm) owned by NASA–Glenn (Changlie Wey). A five-point calibration procedure for NO was conducted for the TILDAS and O_3-chemiluminescence NO instruments before and after the line strength quantification experiment. The sensitivity, hence calibration, of the O_3-chemiluminescence instrument is affected by

Author's personal copy

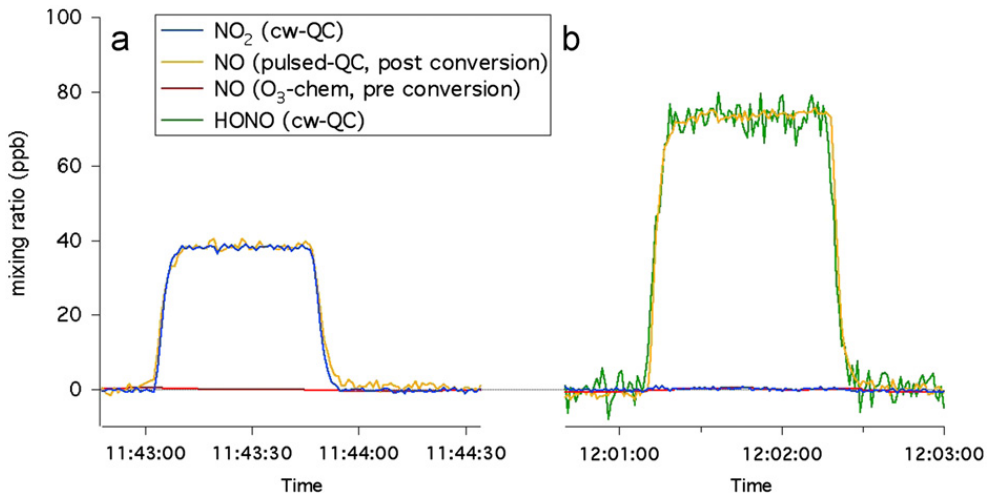

Fig. 2. Time series (1-hertz) of HONO, NO_2 and NO (measured by two different instruments) mixing ratios (ppb) during two gas addition experiments. Addition of (a) NO_2 from a permeation device and (b) generated HONO.

humidity and was taken into account by conducting calibrations at the same water vapor mixing ratio observed during the addition experiments. Output flow rates from a dynamic gas calibrator (ThermoElectron, model 146i) used during NO calibrations were compared to two calibrated (Gilibrator and Bios Dry Cal) flow meters and showed agreement to within 3%. The transducer (MKS, 0–1000 Torr) measuring the pressure inside the sample cell was calibrated at 0 Torr and at ambient pressure using a Hg-manometer.

Fig. 2b shows a brief time series of mixing ratios during an addition of gaseous HONO, generated by flowing UltraPure air (Middlesex gases) first through a gas-washing bottle filled with dilute hydrochloric acid (Sigma Aldrich, 30% wt.) then through a 50 mL round-bottom (1 in. diameter) Pyrex chamber loaded with approximately 5 g sodium nitrite granules (Sigma-Aldrich, 99.999%) where HONO was produced via reaction R_1 [37]. Side products NO and NO_2 likely produced by reaction R_2 accounted for less than 3% by mixing ratio of total HONO and were explicitly taken into account. Nitric acid (HNO_3)–also reducible to NO by molybdenum catalysis–was not directly measured during the experiments. Addition of gaseous HNO_3 from a permeation device and measured as NO following catalytic conversion exhibited a much slower response time through the system due to surface interaction (not pictured) than those exhibited by NO and NO_2 (Fig. 2), gases unlikely to strongly interact with surfaces. We assert negligible amounts of HNO_3 via reaction R_3 were generated alongside HONO, which exhibited response times through the system similar to those of NO and NO_2 (Fig. 2b). We assume nitrosyl chloride (ClNO) was also a negligible contributor due to its slow formation rate [38] and the fact that HONO output levels were positively dependent on the concentration of the HCl solution, indicating HCl was the limiting reagent thus unavailable for reaction R_4 downstream of the $NaNO_2$ chamber. Potential interferences from other reducible nitrogen oxide species such as NO_3, N_2O_4 and N_2O_5 were assumed to be nonexistent due to the short residence times in the system and the absence of an ozone precursor.

$$(R_1)\mathrm{HCl(g)}+\mathrm{NaNO_2(s)}\rightarrow\mathrm{HONO(g)}+\mathrm{H_2O}$$

$$(R_2)\mathrm{HONO(g)}+\mathrm{HONO(ads)}\rightarrow\mathrm{NO(g)}+\mathrm{NO_2(g)}+\mathrm{H_2O}$$

$$(R_3)\mathrm{HONO(g)}+\mathrm{NO_2(g)}\rightarrow\mathrm{NO(g)}+\mathrm{HNO_3(g)}$$

$$(R_4)\mathrm{HCl(g)}+\mathrm{HONO(g)}\rightarrow\mathrm{ClNO(g)}+\mathrm{H_2O}$$

Effective line strengths were calculated by taking into account the total HONO concentration, laser light path length, instrumental line width and sample cell pressure and temperature, using an algorithm called SELECTLINES [39] (Igor Pro, version 4.2, WaveMetrics, Inc.) developed by Aerodyne Research, Inc. The program first determines the line position given an initial guess then calculates the strength of each line by fitting a Voigt line profile to the observed absorbance spectrum. Absolute HONO line positions were determined relative to those of nearby water vapor and/or nitrous oxide along with laser tuning rates determined by recorded spectra of a germanium etalon, all except for experiments conducted when scanning between 1659.25 and 1659.55 cm^{-1} and between 1659.85 and 1660.10 cm^{-1}. In these instances, HONO line positions were based on those obtained from a broadband FTIR spectrum with resolution better than 0.005 cm^{-1} ranging from 700 to 4,000 cm^{-1}, provided by M. Herman (personal communication). The same spectrum provided relative line strengths, which were scaled to absolute line strengths of the *trans* ν_3 mode from the ATMOS database [32], whose strengths are based upon band strengths reported by Kagann and Maki [40]. The resulting line strengths are hereafter referred to as KMH and serve as the basis of comparison to other studies discussed below. The air-broadened half-width at half-maximum (γ_{air}) was obtained by iteratively varying γ_{air} by 0.0010 cm^{-1} atm^{-1} to optimize the spectral fits to each

Author's personal copy

observed spectrum at eight different pressures from 6.6 to 72.1 Torr. All experiments were conducted at 303 K.

3. Results and analysis

The top panels of Figs. 3 and 4 show the observed absorbance spectra (green markers) during HONO addition experiments for the *cis* and *trans* conformers, respectively. Their corresponding least-square non-linear fits (blue lines) using the calculated line strength, line position and γ_{air} values are also presented in the top panels of Figs. 3 and 4. A common γ_{air} value of $0.0980 \pm 0.0050\ \mathrm{cm}^{-1}\ \mathrm{atm}^{-1}$ was obtained for both conformers for all lines scanned.

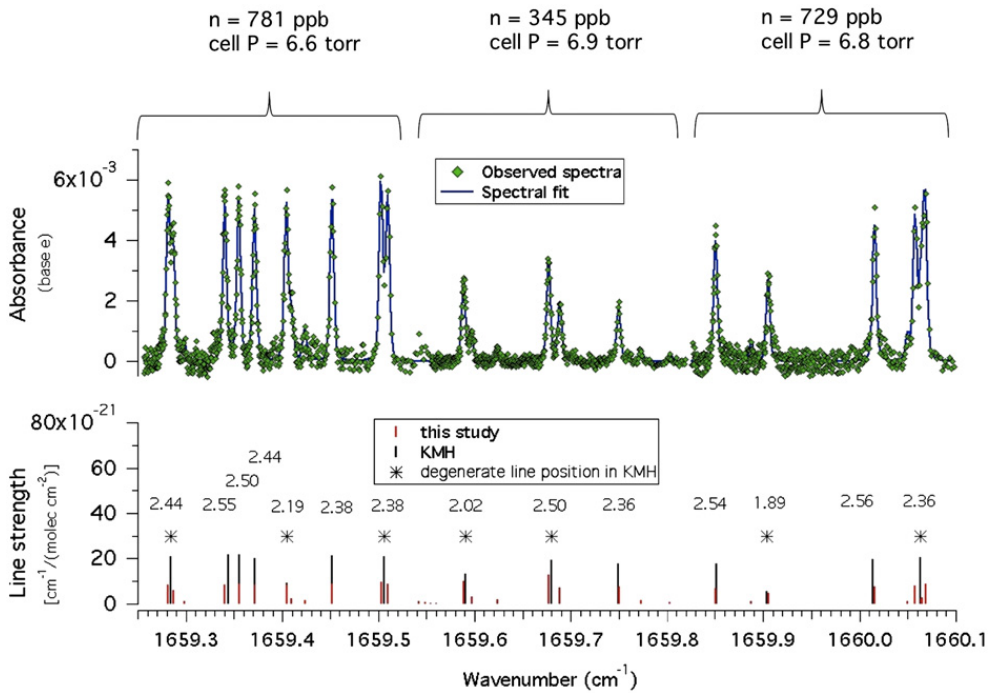

Fig. 3. Absorbance (base e) spectra of *cis*-HONO (top panel) and effective line strengths (bottom panel) from KMH (black) and this study (red), all plotted as a function of wavenumber (cm^{-1}). Listed numbers represent the ratio of KMH strengths to those from this study. Brackets above the figure summarize each experimental condition. Asterisks point to degenerate entries in KMH due to limited spectral resolution. (For interpretation of the references to color in this figure legend, the reader is referred to the web version of this article.)

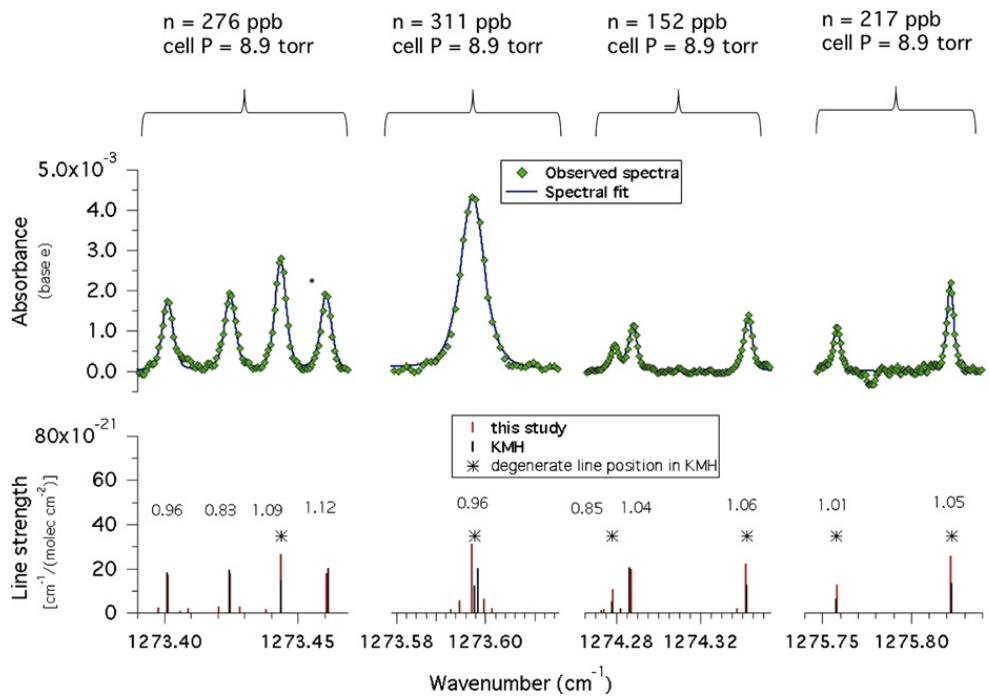

Fig. 4. Same as Fig. 3, for *trans*-HONO.

Author's personal copy

The bottom panels compare our line strengths to those of KMH, described above. Uncertainty in the reported line strengths is less than 6%, estimated by aggregating the errors associated with the accuracy of the NO tank (1%), NO calibration (0.5% in slope), mass flow rate (1% for small head, 2% for large head) and pressure transducer (1%). Tables 1 and 2 list the line position and strengths obtained from this study for the *cis* and *trans* conformers, respectively.

Whereas the cumulative strengths for each of the 10 discernible peaks for the *trans* conformer near 1275 cm^{-1} (Fig. 4, top panel) are on average consistent with those of KMH, the 14 peaks for the *cis* conformer at 1660 cm^{-1} (Fig. 3, top panel) are lower than those of KMH by a factor of approximately 2.4. This discrepancy for the *cis* ν_2 band is likely a result of the difficulty–caused by the presence of lines of interfering species–associated with accurately integrating the broad-band spectrum of Kagann and Maki [40]. Fig. 5 compares two sets of absorbance spectra of the ν_2 bands of *cis* and *trans*-HONO centered around 1640 and 1699 cm^{-1}, respectively. The solid black line represents FTIR observations made by Sharpe et al. [41], who also normalized their broad-band HONO spectrum by the ν_3 band strength value of Kagann and Maki [40]. The dotted gray line is a simulated spectrum generated using the KMH line strengths and positions under the same experimental conditions of Sharpe et al. [41], hereafter referred to as S04. Note the KMH spectrum shows comparable absorbance depths for the ν_2 bands of the *cis* and *trans* conformers, as does the spectrum observed by Kagann and Maki [40] (top panel of their Fig. 3). S04, on the other hand, exhibits absorbance by the *cis* conformer that is about half that of KMH, consistent with observation of this study.

Table 1
Line positions and effective line strengths for *cis*-HONO at 303 K.

Line position (cm^{-1})	Line strength (cm^{-1}/(molec-cm^{-2}) $\times 10^{-22}$)
1659.281714	84.99
1659.286911	61.68
1659.298047	10.49
1659.340462	85.30
1659.354836	86.99
1659.371374	82.90
1659.404336	84.47
1659.409714	24.11
1659.423318	16.95
1659.452315	89.83
1659.503076	95.71
1659.509912	88.10
1659.542224	14.09
1659.549186	8.30
1659.554688	3.54
1659.560453	4.88
1659.588721	101.50
1659.596820	32.83
1659.623827	18.63
1659.676974	129.20
1659.688638	74.19
1659.749633	74.88
1659.772514	15.57
1659.803308	9.34
1659.850733	69.18
1659.887624	11.23
1659.905308	46.62
1660.015667	77.78
1660.050167	13.57
1660.057681	79.63
1660.063576	24.24
1660.064774	28.94
1660.068246	87.64

Table 2
Line position and effective line strengths for *trans*-HONO at 303 K.

Line position (cm^{-1})	Line strength (cm^{-1}/(molec-cm^{-2}) $\times 10^{-22}$)
1273.397922	22.30
1273.401383	168.50
1273.405927	8.29
1273.409133	19.27
1273.420385	29.12
1273.424695	17.63
1273.428455	17.63
1273.438182	15.00
1273.443661	264.80
1273.460643	179.20
1273.593035	15.04
1273.594676	55.26
1273.597142	312.80
1273.599613	63.20
1273.601263	18.53
1274.272566	11.12
1274.274129	16.36
1274.278059	108.10
1274.281960	20.63
1274.286922	197.80
1274.337689	18.62
1274.341812	222.00
1275.758141	125.20
1275.822070	257.00

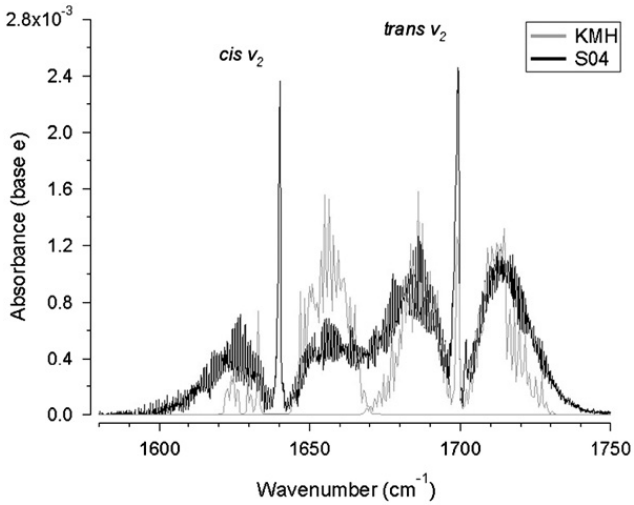

Fig. 5. Absorbance spectra (base e) obtained by S04 (black) and KMH (gray) of the ν_2 bands of *cis* and *trans*-HONO centered around 1640 and 1699 cm^{-1}, respectively. While there is good agreement between the two spectra for the *trans* conformer, the S04 spectrum is lower than that of KMH by about a factor of two for the *cis* conformer.

Author's personal copy

One critical difference between these experiments is the method of generating gaseous HONO. The spectra presented here and by S04 were obtained from a near-pure source of gaseous HONO, generated according to the protocol of Febo et al. [37]. Kagann and Maki [40], on the other hand, obtained HONO as a minor byproduct from the heterogeneous reactions between water vapor and nitrogen oxides sealed in a static vessel. Consequently, spectral subtraction of interfering species was required to obtain the HONO spectrum. We note, for instance, the presence of the much stronger NO_2 absorption structure at the same spectral region as that of the ν_2 band of *cis*-HONO (bottom panel of Fig. 3 in Kagann and Maki [40]). Any biasing errors associated with the NO_2 line shape or concentration would have affected the spectral subtraction, hence, the retrieved HONO band strength. We rule out the difference in *cis*/*trans* ratio resulting from the different way in which gaseous HONO was generated, as the cause of the line/band strength discrepancy for *cis*-HONO. Given an isomerization energy barrier of 9.7 kcal mol^{-1} [42], equilibrium between the two conformers is reached on the order of pico-seconds even in the extreme case that only one conformer is initially generated by the method of Febo et al. [37]. Deviation from *cis*/*trans* equilibrium by infrared light absorption-induced isomerization, likewise, did not play a role since the low energy cutoff occurs around 3,200 cm^{-1} [42].

Our findings are supported by two independent studies [43–45], which validate the ν_3 band strength of the *trans* conformer using its absorption cross section in the ultraviolet region near 340–380 nm. Moreover, ambient observations from the Study of Houston Atmospheric Radical Precursor campaign (Apr–May, 2009) show total HONO measurements using the *cis* absorption lines between 1659.45 and 1659.75 cm^{-1} agree to within 6% of those made by three other independent instruments. Detailed analysis on the HONO inter-comparison is being prepared by J. Pinto et al. (personal communication). The results here, however, are inconsistent with those of Becker et al. [46], which report effective strengths of nine absorption lines near 1255 cm^{-1} (P-branch of *trans* ν_3 mode) that are exactly half of what is expected given the band strengths reported by Kagann and Maki [40] and Maki [47]. The cause for this discrepancy remains undetermined. A key difference between the current study and that of Becker et al. [46] is the way in which gaseous HONO was quantified. Whereas in the present work, HONO was simultaneously measured by complete conversion followed by continuous NO quantification by calibrated absorption spectroscopy, Becker et al. [46] extracted gaseous HONO in a basic liquid trap followed by ion chromatography to quantify the nitrite ion.

Upon rescaling the *cis* ν_2 KMH band using the region between 1650 and 1670 cm^{-1} as a guide to match the S04 spectrum, the values obtained here are still about a factor of 1.4 less than the rescaled KMH line strengths. This is likely due to missing absorption lines resulting from spectral interference in the KMH linelist. This would require scaling existing lines higher than the actual values to compensate for those missing. That there are missing lines in the KMH linelist is evident in the marked difference in the KMH and S04 spectra in the wings of both *cis* and *trans* ν_2 modes (Fig. 5). Lastly, we note the band strengths of Kagann and Maki [40] are based on experimental condition at 296 K, whereas values reported here were obtained at 303 K. Normalizing to the nominal temperature of 296 K–depending on which *cis*/*trans* energy difference is used – changes these values by at most 2%.

4. Improving atmospheric measurements

Our current detection limit (1 s $3-\sigma$) for quantifying total HONO using cw-QC TILDAS is 300 ppt, scanning the *cis* absorption lines near 1660 cm^{-1} and utilizing an astigmatic multi-pass sample cell with a total absorption path length of 210 m at a cell pressure of 30 Torr [27]. In addition to increasing the absorption path length or improving the background electronic noise associated with the detector, sensitivity (i.e. absorbance) can be enhanced by choosing a spectral region in which HONO absorbs light more strongly. In light of our results and using the KMH linelist as a guide, a factor of about 2 improvement in precision can be readily achieved by targeting absorption lines for the *trans* conformer at 1247.16 (P-branch of ν_2 mode) or 1273.60 cm^{-1} (R-branch of ν_2 mode), as these lines are relatively free of spectral interference from water vapor and other known absorbers. Precision (1-s $3-\sigma$) as low as 60 ppt may be obtained under the same conditions with *trans* conformer absorption lines at 1709.00 or 1713.51 cm^{-1} (R-branch of ν_2 mode), for which there is good agreement between the KMH and S04 spectra (Fig. 5).

A targeted line-by-line study such as the one conducted here is likely required, however, for better accuracy in the retrieved HONO concentrations obtained from these less-studied spectral regions. Fig. 4 shows that while on average our *trans*-HONO line strengths agree well with those in the KMH linelist, there may be a difference as high as 17% for a single discernible absorption peak. Discrepancies are more frequent in spectral regions where there is close overlap of absorption lines, pointing to the limited resolution of the KMH linelist. Furthermore, assessments of absorption parameters including the temperature dependence of isomerization and the air-broadened halfwidth are required for remotely measuring HONO and for its inclusion in linelist compilations such as HITRAN [33].

The assertion here that the *cis* ν_2 band strength of Kagann and Maki [40] is too high by a factor of about 2.4 implies that previous measurements of HONO concentrations in aircraft exhaust [31] and references therein, should be adjusted accordingly. Examination of Table 1 of Ref. [31] shows that correction by a factor of 2.4 of the measurements that utilized the *cis* ν_2 band strength [40], brings them closer to the range observed by measurements that used line strengths that are consistent with the *trans* ν_2 [31] and ν_3 [26] band strengths.

5. Conclusion

We report *effective* line strengths for the *cis* and *trans* conformers of HONO. Absorbance of each conformer was

Author's personal copy

recorded using multiple TILDAS systems equipped with cw-QC lasers, while simultaneously quantifying total HONO by catalytic conversion to NO. Line strengths obtained in this study for the *trans* conformer near the 1275 cm^{-1} spectral region are in good agreement with the previously reported *trans* ν_3 band strength [40], confirmed by two independent studies by comparison to the UV absorption cross section [43–45]. Line strengths for the *cis* conformer at 1660 cm^{-1} are, however, lower than reported *cis* ν_2 band strength [40] by about a factor of 2.4. The reason for the *cis* ν_2 line/band strength discrepancy, we submit, is the presence of interfering absorption lines from chemical species other than HONO in the spectra obtained in previous studies [40].

Acknowledgments

This project was funded by the National Science Foundation (Awards nos. AGS–0813617 and 0814202). The authors gratefully acknowledge M. Herman for his contribution of the high resolution FTIR HONO spectrum, and C. Wey for loaning us his NO calibration tank. We would also like to thank J. Kleffmann, T.J. Johnson, S.W. Sharpe and S.D. Wankel for their insights and feedback.

References

[1] Platt U, Perner D, Harris GW, Winer AM, Pitts JN. Observations of nitrous-acid in an urban atmosphere by differential optical-absorption. Nature 1980;285(5763):312–4.
[2] Winer AM, Biermann HW. Long pathlength differential optical-absorption spectroscopy (DOAS) measurements of gaseous HONO, NO_2 and HCHO in the California south coast air basin. Res Chem Intermediates 1994;20(3-5):423–45.
[3] Alicke B, Geyer A, Hofzumahaus A, Holland F, Konrad S, Patz HW, et al. OH formation by HONO photolysis during the BERLIOZ experiment. J Geophys Res-Atmos 2003;108(D4). http://dx.doi.org/10.1029/2001JD000579.
[4] Harris GW, Carter WPL, Winer AM, Pitts JN, Platt U, Perner D. Observations of nitrous acid in the Los Angeles atmosphere and implications for predictions of ozone precursor relationships. Environ Sci Technol 1982;16(7):414–9.
[5] Ren XR, Harder H, Martinez M, Lesher RL, Oliger A, Simpas JB, et al. OH and HO_2 chemistry in the urban atmosphere of New York city. Atmos Environ 2003;37(26):3639–51.
[6] Acker K, Febo A, Trick S, Perrino C, Bruno P, Wiesen P, et al. Nitrous acid in the urban area of Rome. Atmos Environ 2006;40(17):3123–33.
[7] Kleffmann J, Gavriloaiei T, Hofzumahaus A, Holland F, Koppmann R, Rupp L, et al. Daytime formation of nitrous acid: a major source of OH radicals in a forest. Geophys Res Lett 2005;32(L05818). http://dx.doi.org/10.1029/2005GL022524.
[8] Sorgel M, Trebs I, Serafimovich A, Moravek A, Held A, Zetzsch C. Simultaneous HONO measurements in and above a forest canopy: influence of turbulent exchange on mixing ratio differences. Atmos Chem Phys 2011;11(2):841–55.
[9] Zhou XL, Zhang N, TerAvest M, Tang D, Hou J, Bertman S, et al. Nitric acid photolysis on forest canopy surface as a source for tropospheric nitrous acid. Nat Geosci 2011;4(7):440–3.
[10] Beine HJ, Amoroso A, Esposito G, Sparapani R, Ianniello A, Georgiadis T, et al. Deposition of atmospheric nitrous acid on alkaline snow surfaces. Geophys Res Lett 2005;32(L10808). http://dx.doi.org/10.1029/2005GL022589.
[11] Honrath RE, Lu Y, Peterson MC, Dibb JE, Arsenault MA, Cullen NJ, et al. Vertical fluxes of NO_x, HONO, and HNO_3 above the snowpack at Summit, Greenland. Atmos Environ 2002;36(15–16):2629–40.
[12] Zhou XL, Beine HJ, Honrath RE, Fuentes JD, Simpson W, Shepson PB, et al. Snowpack photochemical production of HONO: a major source of OH in the Arctic boundary layer in springtime. Geophys Res Lett 2001;28(21):4087–90.
[13] Spicer CW, Kenny DV, Ward GF, Transformations Billick IH. Lifetimes, and sources of NO_2, HONO, and HNO_3 in indoor environments. J Air Waste Manage Assoc 1993;43(11):1479–85.
[14] Pitts JN, Wallington TJ, Biermann HW, Winer AM. Identification and measurement of nitrous acid in an indoor environment. Atmos Environ 1985;19(5):763–7.
[15] Beckett WS, Russi MB, Haber AD, Rivkin RM, Sullivan JR, Tameroglu Z, et al. Effect of nitrous acid on lung function in asthmatics: a chamber study. Environ Health Perspect 1995;103(4):372–5.
[16] Jarvis DL, Leaderer BP, Chinn S, Burney PG. Indoor nitrous acid and respiratory symptoms and lung function in adults. Thorax 2005;60(6):474–9.
[17] Pitts JN, Grosjean D, Vancauwenberghe K, Schmid JP, Fitz DR. Photooxidation of aliphatic amines under simulated atmospheric conditions: formation of nitrosamines, nitramines, amides, and photochemical oxidant. Environ Sci Technol 1978;12(8):946–53.
[18] Sleiman M, Gundel LA, Pankow JF, Jacob P, Singer BC, Destaillats H. Formation of carcinogens indoors by surface-mediated reactions of nicotine with nitrous acid, leading to potential thirdhand smoke hazards. Proc Nat Acad Sci USA 2010;107(15):6576–81.
[19] Dibb JE, Huey LG, Slusher DL, Tanner DJ. Soluble reactive nitrogen oxides at South Pole during ISCAT 2000. Atmos Environ 2004;38(32):5399–409.
[20] Kleffmann J, Heland J, Kurtenbach R, Lorzer J, Wiesen P. A new instrument (LOPAP) for the detection of nitrous acid (HONO). Environ Sci Pollut Res 2002:48–54.
[21] Park SS, Hong JH, Lee JH, Kim YJ, Cho SY, Kim SJ. Investigation of nitrous acid concentration in an indoor environment using an *in-situ* monitoring system. Atmos Environ 2008;42(27):6586–96.
[22] Zhou XL, Qiao HC, Deng GH, Civerolo K. A method for the measurement of atmospheric HONO based on DNPH derivatization and HPLC analysis. Environ Sci Technol 1999;33(20):3672–9.
[23] Kleffmann J, Lorzer JC, Wiesen P, Kern C, Trick S, Volkamer R, et al. Intercomparison of the DOAS and LOPAP techniques for the detection of nitrous acid (HONO). Atmos Environ 2006;40(20):3640–52.
[24] Liao W, Case AT, Mastromarino J, Tan D, Dibb JE. Observations of HONO by laser-induced fluorescence at the South Pole during ANTCI 2003. Geophys Res Lett 2006;33(L09810). http://dx.doi.org/10.1029/2005GL025470.
[25] Stutz J, Alicke B, Neftel A. Nitrous acid formation in the urban atmosphere: Gradient measurements of NO2 and HONO over grass in Milan, Italy. J Geophys Res Atmos 2002;107(D22):8192, http://dx.doi.org/10.1029/2001JD000390.
[26] Lee BH, Santoni GW, Wood EC, Herndon SC, Miake-Lye RC, Zahniser MS, et al. Measurements of nitrous acid in commercial aircraft exhaust at the alternative aviation fuel experiment. Environ Sci Technol 2011;45(18):7648–54.
[27] Lee BH, Wood EC, Zahniser MS, McManus JB, Nelson DD, Herndon SC, et al. Simultaneous measurements of atmospheric HONO and NO_2 via absorption spectroscopy using tunable mid-infrared continuous-wave quantum cascade lasers. Appl Phys B-Lasers Opt 2011;102(2):417–23.
[28] Li YQ, Schwab JJ, Demerjian KL. Fast time response measurements of gaseous nitrous acid using a tunable diode laser absorption spectrometer: HONO emission source from vehicle exhausts. Geophys Res Lett 2008;35(L04803). http://dx.doi.org/10.1029/2007GL031218.
[29] Schiller CL, Locquiao S, Johnson TJ, Harris GW. Atmospheric measurements of HONO by tunable diode laser absorption spectroscopy. J Atmos Chem 2001;40(3):275–93.
[30] Wood EC, Herndon SC, Timko MT, Yelvington PE, Miake-Lye RC. Speciation and chemical evolution of nitrogen oxides in aircraft exhaust near airports. Environ Sci Technol 2008;42(6):1884–91.
[31] Wormhoudt J, Herndon SC, Yelvington PE, Miake-Lye RC, Wey C. Nitrogen oxide (NO/NO_2/HONO) emissions measurements in aircraft exhausts. J Propul Power 2007;23(5):906–11.
[32] Brown LR, Farmer CB, Rinsland CP, Toth RA. Molecular line parameters for the atmospheric trace molecule spectroscopy experiment. Appl Opt 1987;26(23):5154–82.
[33] Rothman LS, Gordon IE, Barbe A, Benner DC, Bernath PE, Birk M, et al. The HITRAN 2008 molecular spectroscopic database. J Quant Spectrosc Radiat Transf 2009;110(9–10):533–72.
[34] Sironneau V, Flaud JM, Orphal J, Kleiner I, Chelin P. Absolute line intensities of HONO and DONO in the far-infrared and re-determination of the energy difference between the *trans*- and *cis*-species of nitrous acid. J Mol Spectrosc 2010;259(2):100–4.
[35] Nelson DD, Shorter JH, McManus JB, Zahniser MS. Sub-part-per-billion detection of nitric oxide in air using a thermoelectrically

Author's personal copy

cooled mid-infrared quantum cascade laser spectrometer. Appl Phys B-Lasers Opt 2002;75(2–3):343–50.

[36] Angeletti G, Restelli G, Commission of the European Communities. Joint Research Centre. Ispra Establishment., Commission of the European Communities. Directorate-General for Science Research and Development., Physico-chemical behaviour of atmospheric pollutants. In: Proceedings of the fourth European symposium held in Stresa, Italy, 23–25 September 1986; organized within the framework of the Concerted Action COST 611. Air pollution research report 2. 1987, Dordrecht; Boston Norwell, MA, USA: D. Reidel Pub. Co.; (Sold and distributed in the USA and Canada by Kluwer Academic Publishers). xiii. 809 p.

[37] Febo A, Perrino C, Gherardi M, Sparapani R. Evaluation of a high-purity and high-stability continuous generation system for nitrous acid. Environ Sci Technol 1995;29(9):2390–5.

[38] Wingen LM, Barney WS, Lakin MJ, Brauers T, Finlayson-Pitts BJ. A unique method for laboratory quantification of gaseous nitrous acid (HONO) using the reaction $HONO+HCl > ClNO+H_2O$. J Phys Chem A 2000;104(2):329–35.

[39] Harward CN, Baren RE, Parrish ME. Determination of molecular parameters for 1,3-butadiene and propylene using infrared tunable diode laser absorption spectroscopy. Spectrochim Acta Pt A-Mol Bio 2004;60(14):3421–9.

[40] Kagann RH, Maki AG. Infrared-absorption intensities of nitrous acid (HONO) fundamental bands. J Quant Spectrosc Radiat Transf 1983; 30(1):37–44.

[41] Sharpe SW, Johnson TJ, Sams RL, Chu PM, Rhoderick GC, Johnson PA. Gas-phase databases for quantitative infrared spectroscopy. Appl Spectrosc 2004;58(12):1452–61.

[42] Hall RT, Pimentel GC. Isomerization of nitrous acid: an infrared photochemical reaction. J Chem Phys 1963;38(8):1889–97.

[43] Barney WS, Wingen LM, Lakin MJ, Brauers T, Stutz J, Finlayson-Pitts BJ. Infrared absorption cross-section measurements for nitrous acid (HONO) at room temperature. J Phys Chem A 2000;104(8):1692–9.

[44] Barney WS, Wingen LM, Lakin MJ, Brauers T, Stutz J, Finlayson-Pitts BJ. Infrared absorption cross-section measurements for nitrous acid (HONO) at room temperature. J Phys Chem A 2001;105(16):4166; Barney WS, Wingen LM, Lakin MJ, Brauers T, Stutz J, Finlayson-Pitts BJ. Infrared absorption cross-section measurements for nitrous acid (HONO) at room temperature. J Phys Chem A 2000;104A:1692.

[45] Gratien A, Lefort M, Picquet-Varrault B, Orphal J, Doussin JF, Flaud JM. Experimental intercomparison of the absorption cross-sections of nitrous acid (HONO) in the ultraviolet and mid-infrared spectral regions. J Quant Spectrosc Radiat Transf 2009;110(4-5):256–63.

[46] Becker KH, Kleffmann J, Kurtenbach R, Wiesen P. Line strength measurements of *trans*-HONO near 1255 cm^{-1} by tunable diode laser spectrometry. Geophys Res Lett 1995;22(18):2485–8.

[47] Maki AG. High-resolution measurements of the ν_2 band of HNO_3 and the ν_3 band of *trans*-HONO. J Mol Spectrosc 1988;127(1): 104–11.